Int J Thermophys (2012) 33:330–341
DOI 10.1007/s10765-011-1144-2

Corrections for Thermal Expansion in Thermal Conductivity Measurement of Insulations Using the High-Temperature Guarded Hot-Plate Method

Jiyu Wu · Roger Morrell

Received: 5 July 2011 / Accepted: 13 December 2011 / Published online: 31 January 2012

Abstract The anticipation of recently published European product standards for industrial thermal insulation has driven improvements in high-temperature thermal conductivity measurements in an attempt to obtain overall measurement uncertainties better than 5 % ($k = 2$). The two measurement issues that are focused on in this article are the effect of thermal expansion on *in situ* thickness measurement and on determining the metering area at high temperatures. When implementing *in situ* thickness measurements, it is vital to correct the thermal expansion of components in a high-temperature guarded hot plate (HTGHP). For example, in the NPL HTGHP this could cause 3.2 % measurement error for a 50 mm thick specimen at 800 °C. The thermal expansion data for nickel 201 measured by NPL are presented, and the effect of this on the metering area of NPL's heater plate (nickel 201) is discussed.

Keywords High-temperature guarded hot-plate · High-temperature insulation · Nickel 201 · Thermal conductivity · Thermal expansion

1 Introduction

The recently published European product standards for industrial thermal insulation materials require the values of thermal conductivity and/or thermal resistance to be specified with a precision of 1 $\mathrm{mW \cdot m^{-1} \cdot K^{-1}}$. Such a stringent requirement may not be practical for measuring insulation at high temperatures, but a measurement uncertainty of 5 % ($k = 2$) or better would be necessary. However, inter-laboratory comparisons within Europe and North America during the past couple of decades have shown a rather higher level of scatter. These

J. Wu (✉) · R. Morrell
National Physical Laboratory, Hampton Road, Teddington TW11 0LW, UK
e-mail: jiyu.wu@npl.co.uk

intercomparisons have been critically reviewed in the literature [1,2]. Although the high-temperature guarded hot-plate (HTGHP) systems used in these inter-comparisons were of different sizes and configurations, each of them conformed to either its national/regional standards (e.g., EN 12667:2001 [3]) or the international standard ISO 8302:1991 [4].

To resolve the gap between the significant scatter of recent intercomparisons and the stringent uncertainty requirement from the product standards, CEN Technical Committee 89 established a task group within its Working Group 11 to review the present standards and measurement techniques. This has led to the recent development of a new technical specification for high-temperature thermal conductivity measurements, prCEN/TS 15548-1:2007 [5]. As one of the few national metrology institutes participating in CEN/TC89/WG11, NPL is actively reviewing the current measurement standards.

NPL has upgraded its HTGHP facility and is currently able to provide accurate thermal conductivity measurements with overall uncertainties of better than 5.0 % ($k = 2$) at temperatures up to 800 °C. The details of the design, construction, and performance checks of this system have been presented previously [6]. However, the details of some techniques that are used in making corrections were not discussed. For example, when compared with thermal conductivity measurements near room temperature, those at high temperatures require additional corrections to account for the effects of thermal expansion on the measurements. However, this issue has not been addressed systematically in previous publications.

NPL and NIST have used nickel 201 alloy (99 mass% nickel plus cobalt) as the heater plate material in their new generation of GHPs [6,7]. Different high-emissivity coatings have been used to increase the emissivity of nickel 201 plates from ∼0.7 to better than 0.8 at high temperatures. However, thermal expansion data for nickel 201 are scarce in the literature, and data for pure nickel are often used as an alternative. Hence, questions have been raised as to whether or not these thermal expansion data for pure nickel reported in the literature are close enough to the thermal expansion of nickel 201.

In this article, we present thermal expansion data for nickel 201 measured at NPL and comparisons with the thermal expansion data for pure nickel reported in the literature [8,9]. These measured thermal expansion data of nickel 201 can be used to correct the metering area of the heater plates used in the computation of the measured value for the thermal conductivity. We also present in this article the details of the technique that is used to carry out *in situ* thickness measurements of specimens in the NPL HTGHP.

Designers and operators of GHPs can use this *in situ* thickness measurement technique and the thermal expansion data for nickel 201 to make corrections and to reduce their measurement uncertainties, and also to analyze disagreements within intercomparisons. Since the thermal expansion of any coatings applied to a heater plate would need to be well matched, these data for nickel 201 can be used when selecting high-temperature, high-emissivity coatings. These data could also be used for verifying the models that calculate the thermophysical properties of nickel-based alloys [10].

2 Upgraded NPL High-Temperature Guarded Hot Plate

The upgraded NPL HTGHP has been designed for thermal measurements on industrial insulation materials in the temperature range 140 °C to 800 °C and in conformance with ISO 8302:1991, EN 12667:2001, and prCEN/TS 15548-1:2007. Measurements are normally restricted to thermally homogeneous specimens between 25 mm and 60 mm thick and thermal resistances between 0.05 $m^2 \cdot K \cdot W^{-1}$ and 2.0 $m^2 \cdot K \cdot W^{-1}$.

The upgraded NPL HTGHP shown in Fig. 1 is a single-specimen apparatus with heat flowing upward through the specimen. It has a static lower module and a movable upper module. The lower module is sealed at the bottom to prevent air entry which might otherwise cause convective heat transfer in the gap between the edge of the central stack and the edge-guards. The lower module, from top to bottom of the central stack, consists of: a main heater-plate, an insulation block, an auxiliary guard-plate, two insulation blocks, and a lower chilled cold-plate. A lower edge-guard surrounds the main heater-plate, the auxiliary guard-plate, and the insulation block between them. The upper module is telescopic, and from bottom to top of the central stack, consists of: a heated cold-plate, two blocks of insulation, and an upper chilled cold-plate. The upper module sits on top of the specimen with its entire weight resting on the specimen that is placed on the main heater-plate. An upper edge-guard surrounds the specimen and the heated cold-plate. The upper module can be lifted to allow a specimen to be loaded between the main heater-plate and the heated cold-plate. With the specimen in position, the upper module can be lowered and the telescopic arrangement allows

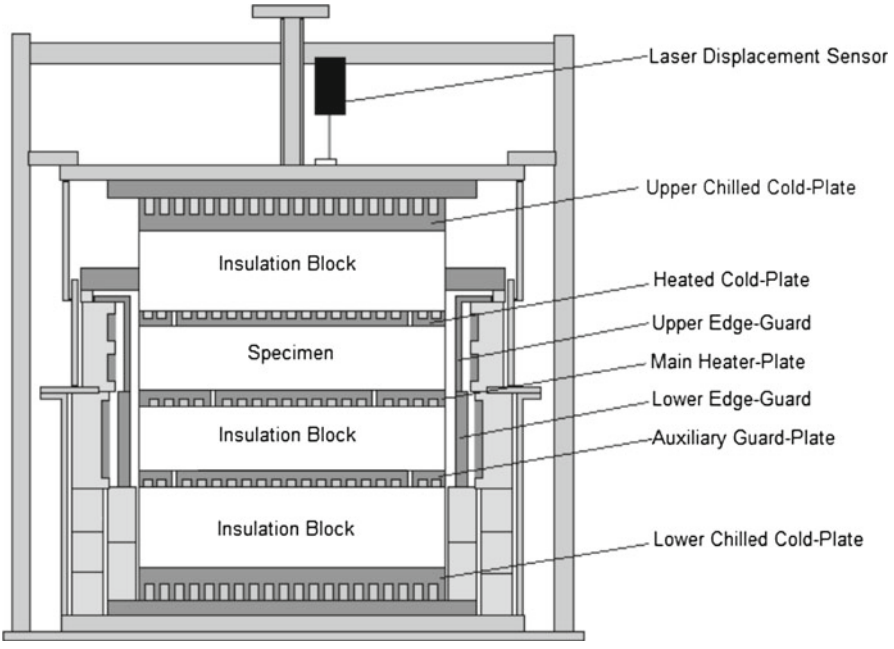

Fig. 1 Schematic diagram of the upgraded NPL HTGHP

the upper edge-guard to surround the specimen and the heated cold-plate. The gap between the edge of the specimen stack and the edge-guards is about 10 mm and is filled with high-density fiber blanket. A laser displacement sensor is mounted on an independent rigid frame above the upper chilled cold-plate to measure the *in situ* thickness of the specimen.

The heater-plate consists of a central heater and a lateral guard heater that are separated by a guard/center gap. The area that is bounded by the middle of the guard/center gap is referred to as the metering area. The determination of the thermal conductivity and thermal resistance by the GHP method involves the measurement of the temperature difference between the opposite faces of a parallel-faced specimen at steady-state when a constant, unidirectional heat flux density of known magnitude passes normally through it. The specimen surface temperatures are measured by thermocouples embedded in the heater plates. The rate of the heat flux density used in calculating the thermal conductivity is determined from the power supplied to the central heater and the metering area of the heater-plate. At steady-state, the thermal conductivity, λ, of the specimens at the mean test temperature is given by

$$\lambda = \frac{Q}{A(T_\mathrm{h})} \times \frac{t(T_\mathrm{m})}{(T_\mathrm{h} - T_\mathrm{c})}, \tag{1}$$

where Q is the power supplied to the central heater of the heater plate (W), T_h is the mean temperature of the specimen hot face (°C), T_c is the mean temperature of the specimen cold face (°C), T_m is the mean specimen temperature (°C), $A(T_\mathrm{h})$ is the metering area of the heater plate at temperature $T_\mathrm{h}(\mathrm{m}^2)$, and $t(T_\mathrm{m})$ is the specimen thickness at the mean specimen temperature $T_\mathrm{m}(\mathrm{m})$.

Uncertainties in overall measurement have been dealt with previously [6]. The focus of this article is the correction for thermal expansion on the *in situ* specimen thickness measurements, $t(T_\mathrm{m})$, and on the metering area, $A(T_\mathrm{h})$.

3 *In Situ* Thickness Measurement, $t(T_\mathrm{m})$

3.1 Requirements and Methods

The laser displacement sensor that is used for *in situ* thickness measurements is calibrated using gauge blocks at room temperature, and its signal output, L, is then converted into distance and used to directly measure the distance between the head of the laser displacement sensor and a central point on the top of the upper chilled cold-plate. Since the central stack is free to move at the top, there is a change in L from its value when the specimen stack is at room temperature $L(25)$ to its value $L(T_\mathrm{m})$ when a thermal conductivity measurement is being made with a mean specimen temperature T_m. This change, $L(T_\mathrm{m}) - L(25)$, results from the thermal expansions/contractions of the specimen, $\Delta L_\mathrm{s}(T_\mathrm{m})$ and the rest of the central stack, $\Delta L_\mathrm{HTGHP}(T_\mathrm{m})$,

$$\Delta L_\mathrm{s}(T_\mathrm{m}) = L(T_\mathrm{m}) - L(25) - \Delta L_\mathrm{HTGHP}(T_\mathrm{m}). \tag{2}$$

To determine $\Delta L_{\mathrm{HTGHP}}(T_{\mathrm{m}})$, three pieces of Herasil 3$^{\mathrm{TM}}$ quartz glass (from Heraeus Quarzglas GmbH & Co. KG) blocks were used as rigid spacers and were embedded evenly in a fiber blanket to make a specimen that is 305 mm in diameter by 50 mm high. Each of the quartz glass blocks is 53 mm in diameter by 50 mm high and has a mean thermal expansion coefficient of about 5×10^{-7} K^{-1} over the temperature range from 0 °C to 900 °C. This is at least an order of magnitude less than the mean thermal expansion coefficient of other materials used in the NPL HTGHP, and therefore its thermal expansion could be neglected as a secondary correction. After the spacers were installed and the system reached equilibrium at room temperature 25 °C, $L_{\mathrm{HTGHP}}(25)$ was recorded first, then the HTGHP was heated to a mean specimen temperature, T_{m}, with a temperature drop of 50 K between the main heater-plate and the heated cold-plate. The value of $L_{\mathrm{HTGHP}}(T_{\mathrm{m}})$ was recorded when the system reached equilibrium again. The thermal expansion of the upgraded HTGHP becomes

$$\Delta L_{\mathrm{HTGHP}}(T_{\mathrm{m}}) = L_{\mathrm{HTGHP}}(T_{\mathrm{m}}) - L_{\mathrm{HTGHP}}(25). \tag{3}$$

For a specimen to be measured in the HTGHP, its thickness at room temperature, $t(25)$ can be measured directly with calibrated callipers or calculated from the signal output of the calibrated laser displacement sensor $L(25)$. The *in situ* thickness of the specimen, $t(T_{\mathrm{m}})$, for use in Eq. 1 can be obtained with a resolution of 50 μm:

$$t(T_{\mathrm{m}}) = t(25) + f[\Delta L_{\mathrm{s}}(T_{\mathrm{m}})], \tag{4}$$

where f is the calibration curve of the laser displacement sensor that converts the change of the laser signal output into distance change.

3.2 Results

The measured values of $\Delta L_{\mathrm{HTGHP}}(T_{\mathrm{m}})$ are plotted in Fig. 2 against mean specimen temperatures from room temperature up to 800 °C with the temperature difference between the hot and cold plates kept at 50 K. Figure 2a shows that when the mean specimen temperature increases from room temperature to 800 °C, the signal output from the laser displacement sensor decreases by −65 mV from its output at room temperature. From the calibration curve shown in Fig. 2b, one can see that this −65 mV change of the laser displacement sensor output signal equals a −1.6 mm change of distance. The negative polarity means the distance between the laser displacement sensor and the top of the upper chilled cold-plate reduces because the central stack of the HTGHP expands.

Therefore, at NPL we correct the thermal expansion of the HTGHP, $\Delta L_{\mathrm{HTGHP}}(T_{\mathrm{m}})$, when carrying out *in situ* thickness measurements. If the thermal expansion of the HTGHP, $\Delta L_{\mathrm{HTGHP}}(T_{\mathrm{m}})$, is not corrected from the signal output change of the laser displacement sensor during an *in situ* thickness measurement at high temperatures, then it would cause a 3.2 % measurement error for a 50 mm thick specimen at 800 °C.

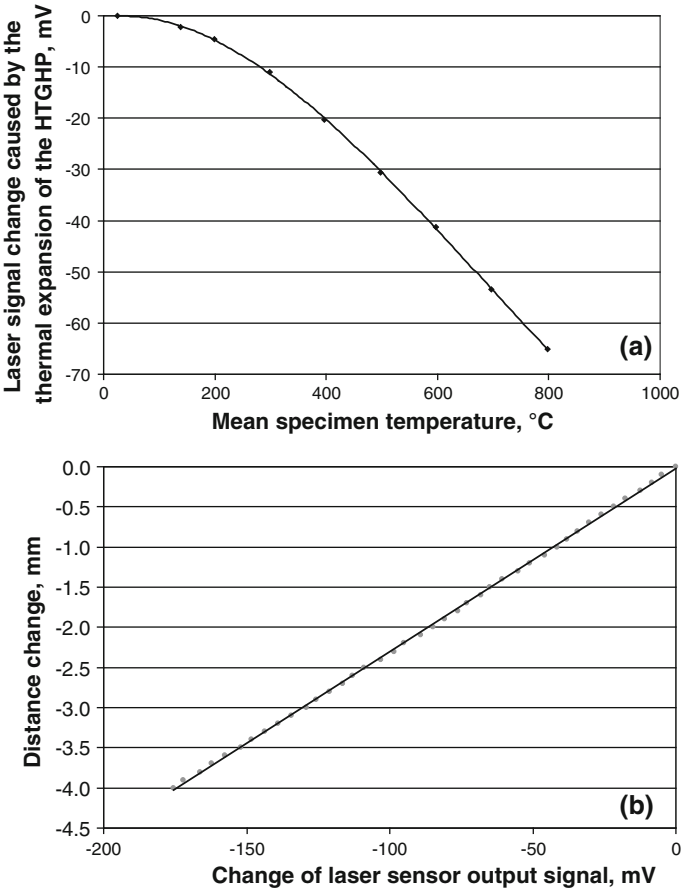

Fig. 2 (a) Thermal expansion of the upgraded NPL HTGHP ($\Delta T = 50$ K) and (b) calibration of laser sensor at room temperature

4 Thermal Expansion of the Metering Area, $A(T_h)$

4.1 Requirements

The metering area of a HTGHP heater plate increases as the temperature is raised. The metering area of the heater plate is given as

$$A(T_h) = \pi D(T_h)^2/4, \tag{5}$$

where $D(T_h)$ is the diameter of the metering area that is bounded by the middle of the center/guard gap. The effect of thermal expansion of the nickel 201 heater plate on the metering area $A(T_h)$ is therefore,

$$\frac{\Delta A(T_h)}{A(T_h)} = 2\frac{\Delta D(T_h)}{D(T_h)}, \tag{6}$$

i.e., twice the linear thermal expansion of the metering area diameter. As a result of the lack of accurate thermal expansion data in the literature, we have measured the thermal expansion of the nickel 201 alloy.

4.2 Measurement Method

A bar test-piece about 30 mm in length and 4 mm square cross section was used as a specimen in the thermal expansion measurements using mechanical dilatometry [11]. The specimen was tested in a modified Linseis dilatometer. The instrument operates in the horizontal mode with a specially constructed alumina apparatus comprising a tube with an end flat against which the test-piece is pushed by an alumina push-rod. The push-rod transmits the changes in length to a linear displacement transducer as the test-piece is heated and cooled. The temperature of the test-piece is measured using a type R thermocouple, and the outputs of the thermocouple and the transducer are recorded at 1 min intervals on a data logger for later analysis.

The instrument is calibrated in the following manner: the alumina test-piece holder is removed, and replaced by a drum micrometer that is used to move the push-rod a prescribed distance. In this way, the absolute sensitivity of the transducer may be determined. The apparatus is reassembled and run over the required temperature range with an alumina test-piece of the same material as the push-rod, and any shift of the baseline output, corresponding to differential temperature distributions in the specimen support and push-rod, is determined. This is used to correct the output from testing an unknown. The correction for the thermal expansion of the apparatus itself may be determined by inserting a certified reference specimen, normally SRM 739, Fused Silica from the National Institute for Standards and Technology, USA or a platinum reference test-piece for high temperatures. The in-house technical procedure and calibration follows measurement standards EN 821-1 and ASTM E228.

The overall uncertainty of the measurement is dependent on the mechanical and microstructural stability of the specimen in the apparatus. Assuming complete stability, the measurement uncertainty when evaluating an unknown test-piece is considered to be $\sim 2\ \%$ ($k = 2$) in $\Delta L/L$ or $0.2 \times 10^{-6}\,\mathrm{K}^{-1}$ ($k = 2$) in the mean coefficient of expansion over a 100 °C temperature range. This uncertainty arises because of the instrument calibration uncertainties, test-piece thermal mass effects, and the repeatability of the mechanical displacement recorded by a simple displacement transducer.

The tests were run at $2\,^{\circ}\mathrm{C} \cdot \mathrm{min}^{-1}$ to a maximum temperature of about 1004 °C in an argon atmosphere. Three thermal cycles were made on the test-piece.

4.3 Results and Discussion

A plot of fractional length change in parts per million (ppm) as a function of temperature in the second thermal cycle is shown in Fig. 3. In the first thermal cycle, there was a test-piece annealing effect taking place leading to a small negative offset between heating and cooling. The data from this cycle were ignored in favor of those from the

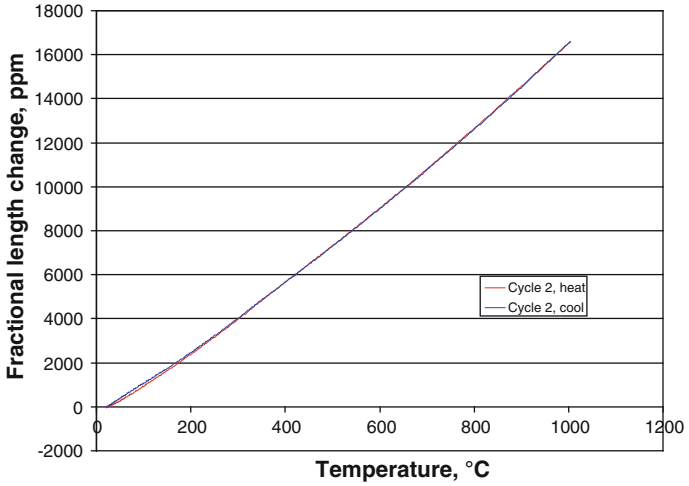

Fig. 3 Fractional length change in parts per million as a function of temperature for the second thermal cycle

second and third cycles, which were averaged to produce the numerical data shown in Table 1. These data show that the effect of thermal expansion on the diameter of the metering area of a nickel 201 heater plate, $\Delta D(T_h)/D(T_h)$, is 1.26 % at 800 °C. From Eq. 6, the effect of thermal expansion on the metering area $\Delta A(T_h)/A(T_h)$ is 2.6 % at 800 °C. Therefore, at NPL we correct the effect of thermal expansion on the metering area.

For the purpose of comparison, in Fig. 4 we have plotted the differences between the reported thermal expansion data for pure nickel in the literature [8,9] and the NPL measured data for nickel 201. The diamond symbols are the difference between the data reported in [8] and the measured data. The difference is within 2 % at temperatures from 320 °C to 850 °C, but at temperatures below 320 °C, the difference increases quickly and reaches 6 % at 150 °C. The square symbols represent the difference between the data reported in [9] and the measured data. This difference is within 2 % in the temperature range 150 °C to 850 °C. The data reported in [9] are closer to the measured thermal expansion data of nickel 201 than the data in [8]. However, it should be noted that up to 150 °C, these differences are approaching the stability and resolution limits of high-temperature mechanical dilatometers.

In addition to the small differences mentioned above, the maximum difference of 6 % between the thermal expansion data for pure nickel [8] and the measured data for nickel 201 only affects the 0.01 % (6 % × 0.17 %) correction of the metering area at temperatures up to 150 °C, whereas at 800 °C, the correction is 2.6 % with lower uncertainty. Therefore, this difference is a secondary factor and does not significantly affect the thermal conductivity measurement uncertainty. Nevertheless, we recommend the use of the measured thermal expansion data of nickel 201 when selecting the high-temperature, high-emissivity coatings for the nickel 201 heater plates.

Table 1 Measured thermal expansion data for nickel 201 alloy (reference temperature: 25 °C)

Temperature (°C)	$\Delta D(T_h)/D(T_h)$ (%) Measured values, Ni 201
25	0
50	0.031
100	0.098
150	0.168
200	0.240
250	0.320
300	0.397
350	0.481
400	0.563
450	0.645
500	0.728
550	0.812
600	0.898
650	0.985
700	1.075
750	1.166
800	1.259
850	1.354
900	1.451
950	1.546
1000	1.647

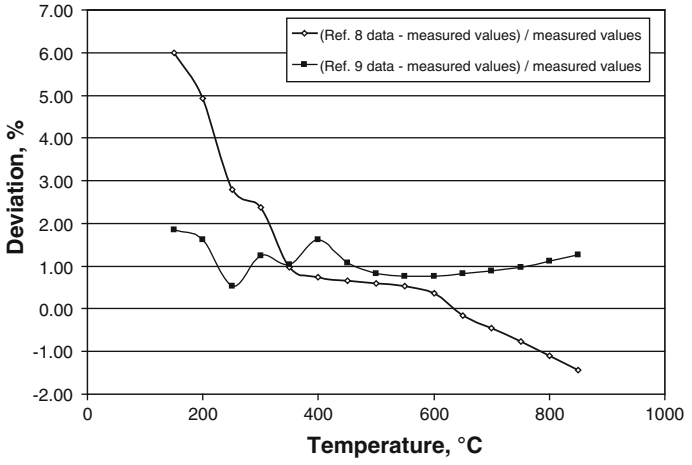

Fig. 4 Deviations of the thermal expansion data for pure Ni in [8,9] from the NPL measured values of nickel 201 alloy

4.4 Inflection in the Thermal Expansion of Nickel 201 Alloy

It was reported in [9] that there was an inflection in the thermal expansion trend for pure nickel at around 300 °C due to a second-order magnetic transition. Close inspection of the measured fractional length change plots reveals a slight meander that is barely noticeable in Fig. 3. To evaluate this in more detail, the fractional length change data on cooling in the first thermal cycle were curve fitted (see Fig. 5), and the expansivity was determined by differentiating the fit. This shows a broad maximum at about 320 °C (see Fig. 6).

It is clear that using such a polynomial fit inevitably smoothes out any peak at the phase transition. Another possible reason would be that nickel 201 is an alloy that contains a small percentage of alloying components, which might also change the phase

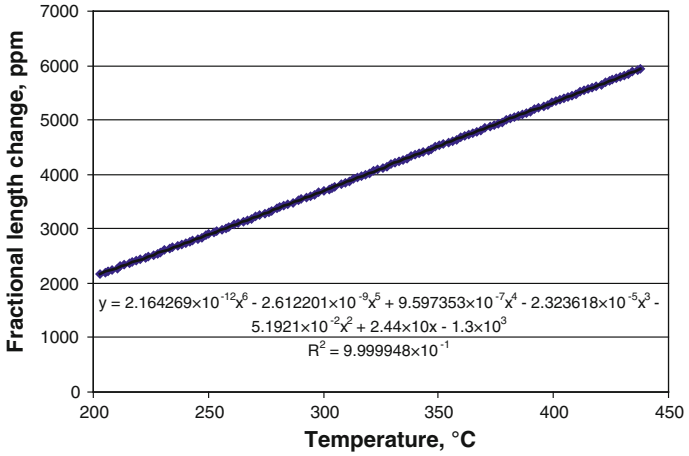

Fig. 5 Fractional length change as a function of temperature in the range 200 °C to 450 °C during cooling in the first cycle, with the six-term polynomial

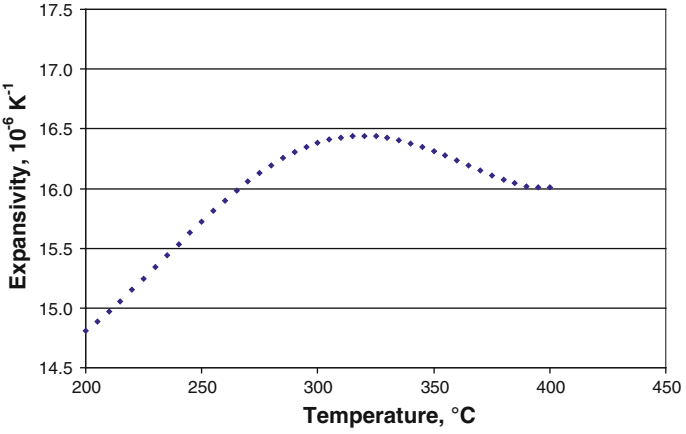

Fig. 6 Expansivity computed from the curve fit in Fig. 5 by differentiation, showing a peak at about 320 °C

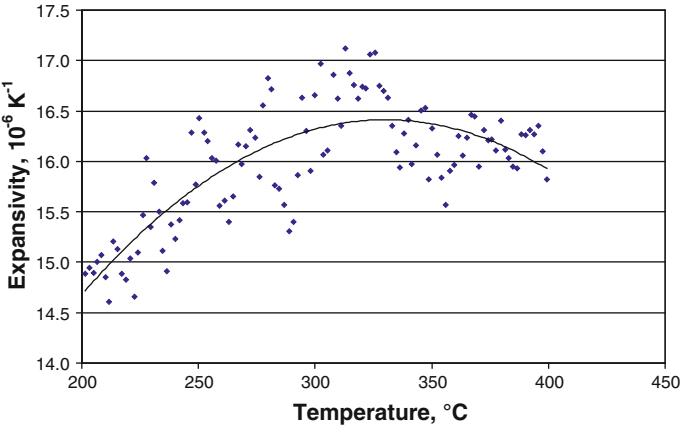

Fig. 7 Expansivity computed by averaging the raw data over five logged points to produce a smoothed data set and the local slope, showing a peak at about 325 °C

change temperature and might modify the shape of the peak. A second approach was tried in which the expansivity was computed as the slope between pairs of fractional length change and temperature data points. Unfortunately, noise limitations in the displacement transducer and data logger system resulted in significant scatter. To smooth the raw data, averages over successive sets of five data points were taken, and the expansivity computed. The result is shown in Fig. 7, where there does indeed appear to be a peak at around 320 °C, but the polynomial fit through the scatter reveals, again, only a maximum at around 325 °C.

However, from the point of view of providing corrections to thermal conductivity data, the thermal expansion data in Table 1 should be adequate, because the effect of the transition is small and barely noticeable in the averaged expansion data.

5 Conclusions

At NPL, we have applied corrections to the effects of thermal expansion on thermal conductivity measurements using a GHP at high temperatures. In this article, we have focused on the effect of the thermal expansion on the *in situ* thickness measurement of the test specimen and on the metering area of a nickel 201 heater plate. After correcting the effect of thermal expansion, the overall measurement uncertainties are better than 5.0 % ($k = 2$).

We have presented details of a technique that can be used in the *in situ* thickness measurement of a thermal conductivity specimen. This method involves measuring the distance change compared to a central reference point at the top of the chilled cold-plate (see Fig. 1) and then calculating the *in situ* specimen thickness. At NPL, we correct the thermal expansion of the HTGHP components, $\Delta L_{\mathrm{HTGHP}}(T_{\mathrm{m}})$. Otherwise, it could cause a 3.2 % measurement error for a 50 mm thick specimen at 800 °C.

We have also presented the NPL measured thermal expansion data for nickel 201 and comparisons with data for pure nickel reported in the literature [8,9].

The measured data for nickel 201 are used to correct the metering area of the heater plates in our HTGHP. The effect of thermal expansion on the diameter of the metering area, $\Delta D(T_h)/D(T_h)$, is 1.26 % at 800 °C, and hence the effect of thermal expansion on the metering area, $\Delta A(T_h)/A(T_h)$, is 2.6 % at 800 °C. If a correction was not applied, then this could contribute a significant upward bias on test results.

The maximum difference between the thermal expansion data for pure nickel reported in the literature [8,9] and the NPL measured data for nickel 201 is 6 % up to 150 °C, reducing to about 2 % up to 800 °C, although the data reported in [9] are closer to the measured thermal expansion data of nickel 201. Since it is only a secondary factor in the correction of the effect of the thermal expansion on the metering area, this difference does not have a significant effect on the thermal conductivity measurement uncertainty. However, we recommend the use of the measured thermal expansion data of nickel 201 when selecting the high-temperature, high-emissivity coatings for matching to the nickel 201 heater plates.

Acknowledgment This study was funded by the National Measurement Office of UK.

References

1. D. Salmon, R. Tye, N. Lockmuller, Meas. Sci. Technol. **20**, 015101 (2009)
2. D. Salmon, R. Tye, N. Lockmuller, Meas. Sci. Technol. **20**, 015102 (2009)
3. EN 12667:2001. European Standard: Thermal performance of building materials and products—determination of thermal resistance by means of guarded hot plate and heat flow meter methods—products of high and medium thermal resistance (2001)
4. ISO 8302:1991. International standard: Determination of steady-state thermal resistance and related properties—Guarded Hot Plate Apparatus (1991)
5. prCEN/TS 15548-1:2007. European Technical Specification: Thermal insulation products for building equipment and industrial installations—determination of thermal resistance by means of the guarded hot plate method—Part 1: measurements at elevated temperatures from 100 °C to 850 °C (2007)
6. J. Wu, D. Salmon, N. Lockmuller, C. Stacey, in *Proceedings of Thermal Conductivity 30/Thermal Expansion 18* (DEStech Publications, Inc., Lancaster, PA, 2010), pp. 529–541
7. R. Zarr, D. Flynn, J. Hettenhouser, N. Brandenburg, W. Healy, in *Proceedings of Thermal Conductivity 28/Thermal Expansion 16* (DEStech Publications, Inc., Lancaster, PA, 2006), pp. 235–245
8. Y. Touloukian, R. Kirby, R. Taylor, P. Desai (eds.), *Thermophysical Properties of Matter, The TPRC Data Series, vol. 12: Thermal Expansion-Metallic Elements and Alloys* (Plenum Publishing Co., New York, 1975), p. 225
9. T. Kollie, Phys. Rev. B **16**, 4872 (1977)
10. K. Mills, Y. Youssef, Z. Li, Y. Su, ISIJ Int. **46**, 623 (2006)
11. J. Valentich, *Tube Type Dilatometers* (Instrument Society of America, Research Triangle Park, NC, 1981)